

Multiple Coexisting Attractors in a Generalized Chua's Circuit with a Smoothly Adjustable Symmetry and Nonlinearity

Tsafack N^{*1,2} and Kengne J¹

¹Department of Electrical Engineering, IUT-FV Bandjoun, University of Dschang, Cameroon

²Department of Physics, University of Dschang, P. O. Box 67, Dschang, Cameroon P.O. Box 67, Dschang Cameroon

Abstract

A generalized Chua's circuit with a single parametric nonlinearity is introduced in this letter. The circuit is obtained by replacing the Chua's diode of the classical Chua's circuit with a parametric active diode pair. The obtained circuit can be described by three differential equations. Preliminary dynamic properties of the circuit are categorized with respect to its parameters and it is found that the circuit has two nonzero stable node-foci leading to complex coexisting behaviours. A plethora of coexisting symmetric and asymmetric attractors are depicted. More importantly, the symmetry of the circuit can be monitored with a single parameter k (i.e. a single control resistor). Also, multistability in the symmetry boundary is discussed by monitoring the single bifurcation parameter k . Finally, Pspice circuit implementation results are consistent with the complex dynamic behaviours observed during numerical analysis.

Keywords: Generalized Chua's circuit; Adjustable nonlinearity; Coexisting bifurcations; Symmetry analysis; Coexisting multiple attractors

Introduction

During the past few years many researchers in the field of nonlinear dynamics are devoted to multistability [1-13]. This is mainly due to its numerous applications in various domains [14-17]. Multistability can be viewed as the coexistence of multiple disconnected attractors in a system's phase space by switching the initial states. In systems presenting such behaviour, the trajectories converge to a basin of attraction given a set of system initial conditions; and the dimension of the basin is very close to the dimension of the state space. Multistability has been previously observed in various dynamical systems including the Chua's circuit [18-26]. Chua's circuit is one of the simplest chaotic circuits with a very rich dynamics reported in the literature. It consists of a linear inductor, a linear resistor, two linear capacitors and a nonlinear part called the Chua's diode. The latter is the only element responsible of the complex dynamics of the circuit. Since the invention of this circuit by Leon O. Chua in 1983, many related works have been reported by modifying the nonlinear part of the circuit. Consequently, Chua's diode has been implemented using standard components such as diode, transistor, operational amplifier and cellular neural network (CNN) just to name a few [27-32]. Most often the obtained system is symmetric and the related attractors are symmetric in the phase space, leading to the coexistence of multiple attractors. A question can then be asked: what is the effect of an asymmetric Chua's diode on the multi-stable behaviour of a system in general and on a Chua's circuit in particular? In other words what are the mechanisms that occur when the Chua's circuit loses its symmetry property in the multi-stable region? This question is very important since the answer leads to the generalization of multistability in the Chua's circuit by adjusting its nonlinear part and hence its symmetry property.

To provide some answer to this question we propose in this paper a generalized Chua's circuit with a smoothly adjustable symmetry and nonlinearity. The circuit is obtained by replacing the nonlinear hyperbolic function $f(x) = -ax + b \sinh(x)$ of a Chua's circuit by its parametric form $f_k(x) = -ax + 0.5b(\exp(kx) - \exp(-x))$ [33]. Let us stress that the nonlinear hyperbolic function $f(x) = -ax + b \sinh(x)$ is a symmetric nonlinear function obtained from an active diode pair. This

nonlinear function has been used by to construct a symmetric system with complex coexisting behaviour of multiple kinds of disconnected symmetric attractors of stable point attractors, limit cycle and chaotic attractors. Earlier, Chen and collaborators used the same active diode pair to construct a Chua's circuit characterized by hidden dynamics and multistability [33,34]. However the coexisting attractors reported in were symmetric due to the symmetric nonlinear function of the model [21-33]. This paper provides an improved Chua's circuit based on a new active diode pair. This active diode pair has the particularity that the form of its nonlinearity is adjustable and hence its symmetry. We then report from the circuit some striking dynamics including reverse bifurcation, merging crisis, coexisting bifurcations leading to coexisting attractors. More importantly, multistability in the symmetry boundary is discussed by switching the control parameter k .

The rest of the paper is structured as follows: Sect. 2 focuses on the description of the improved Chua's circuit with adjustable nonlinearity. The equilibrium point and their stability are investigated through the dimensionless equation. Bifurcation analysis of the circuit is done in Sect. 3. Sect. 4 is devoted to Pspice and experimental results. The work is summarized in Sect. 5.

Description and Analysis of the Generalized Chua's Circuit

The circuit and state equations

The generalized Chua's circuit is presented in the schematic diagram (Figure 1). Like the classical Chua's circuit it consists of a linear inductor L , two linear capacitors C_1 and C_2 , a linear resistor R

***Corresponding author:** Tsafack N, Department of Electrical engineering, IUT-FV Bandjoun, University of Dschang, Cameroon, Tel: +237697876234; E-mail: nestor.tsafack@yahoo.fr

Received December 21, 2018; **Accepted** April 05, 2019; **Published** April 12, 2019

Citation: Tsafack N, Kengne J (2019) Multiple Coexisting Attractors in a Generalized Chua's Circuit with a Smoothly Adjustable Symmetry and Nonlinearity. J Phys Math 10: 298. doi: [10.4172/2090-0902.1000298](https://doi.org/10.4172/2090-0902.1000298)

Copyright: © 2019 Tsafack N, et al. This is an open-access article distributed under the terms of the Creative Commons Attribution License, which permits unrestricted use, distribution, and reproduction in any medium, provided the original author and source are credited.

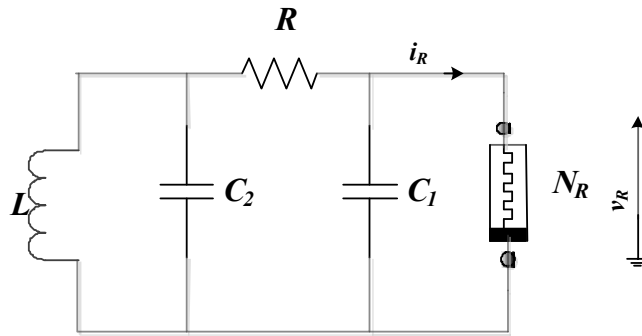


Figure 1: The modified Chua's circuit consist of a linear inductor L, two linear capacitor C₁ and C₂, a linear resistor R.

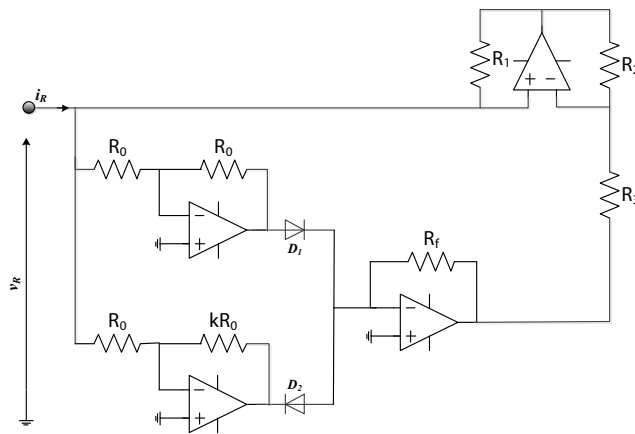


Figure 2: The nonlinear resistor N_r of the modified Chua's circuit.

and a parametric Chua's diode N_r (Figure 2). Let us mention that an adjustable resistor R_k=kR₀ is introduced into the Chua's diode in order to smoothly adjust its symmetry making the circuit to be generalized. Therefore the symmetry of the circuit can be established for k=1(i.e R_k=R₀). When k ≠ 1, (i.e R_k≠R₀) the symmetry breaks down.

To derive the mathematical model of the circuit it is necessary to assume that all circuit's components operate in the linear region except the semiconductor diodes. The latter are modeled with an exponential function given by the Shockley diode equation [34,35]:

$$i_d = i_{d1} - i_{d2} = I_s \left[\exp\left(-\frac{v_{d1}}{nV_T}\right) - 1 \right] - I_s \left[\exp\left(\frac{R_0}{R_k} \frac{v_{d1}}{nV_T}\right) - 1 \right] \quad (1)$$

$$i_d = -2I_s \left[\exp\left(\frac{R_0}{R_k} \frac{v_R}{nV_T}\right) - \exp\left(-\frac{v_R}{nV_T}\right) \right] \quad (2)$$

Where I_s is the reverse saturation current, n is the emission coefficient, and V_T is the thermal voltage of the diode [36-40]. Assuming v_r=v_i and i_r the voltage across and the current through the Chua's diode, the characteristics can be derived as follows

$$i_R = -\frac{v_R}{R_3} + \frac{R_f I_s}{R_3} \left[\exp\left(\frac{R_0}{R_k} \frac{v_R}{nV_T}\right) - \exp\left(-\frac{v_R}{nV_T}\right) \right] \quad (3)$$

With the above considerations, the dynamics of the generalized Chua's circuit is characterized by a set of three coupled first order nonlinear differential equations:

$$\begin{cases} C_1 \frac{dv_1}{dt} = \frac{1}{R}(v_2 - v_1) - i_R \\ C_2 \frac{dv_2}{dt} = \frac{1}{R}(v_1 - v_2) + i_L \\ L \frac{di_L}{dt} = -v_2 \end{cases} \quad (4)$$

The circuit can be rescaled to its dimensionless form (6) with the following change of variables and parameters (5):

$$x_1 = \frac{v_1}{nV_T}; \quad x_2 = \frac{v_2}{nV_T}; \quad x_3 = \frac{Ri}{nV_T}; \quad t = \frac{t}{RC} \quad (5)$$

$$a = \frac{R}{R_3}; \quad b = \frac{RI_s}{nV}; \quad \alpha = \frac{C_2}{C_1}; \quad \beta = \frac{R}{L} \frac{C_2}{C_1}; \quad k = \frac{R_k}{R_0}$$

$$\begin{cases} \dot{x}_1 = \alpha(x_2 - x_1) - \alpha f_k(x_1) \\ \dot{x}_2 = x_1 - x_2 + x_3 \\ \dot{x}_3 = -\beta x_2 \end{cases} \quad (6)$$

Where f_k(x₁)=-ax₁+b(exp(kx₁)-exp(-x₁)) is the nonlinear characteristic of the Chua's diode. Remark that only one state variable is concerned with the nonlinear part of the model. This adjustable nonlinearity is responsible of the complex dynamics of the whole system. Five parameters (k; a; α; β) can be identified in the model. One of them (b) is related to the intrinsic diodes parameters and will be

kept constant ($b=3.01756 \times 10^{-4}$) during the numerical simulations. The rest can be used as control parameter but α and k are used as the main control parameters. Note that parameter k is used to study the effect of symmetry in a multi-stable region.

Symmetry

By switching parameter k the symmetry of the generalized Chua's circuit can be modified (Figure 2) is the representation of the nonlinear function $f_k(x)$ where the symmetry breaks with the variation of parameter k . The curve in black is related to the particular case $k=1$. This particular case has been extensively studied by Bao and coworkers [33]. For this case the nonlinear function is symmetric and the system is invariant under the coordinate transformation $(x_1, x_2, x_3) \Leftrightarrow (-x_1, -x_2, -x_3)$ leading to symmetric attractors, but in the general case this condition can only be achieved by switching a parameter (k) related to the nonlinearity.

Fixed point analysis

The equilibrium points of the system can be evaluated by setting the right hand side of (6) to zero. It is found that system (6) has three equilibrium points including one zero equilibrium and two non-zero equilibrium points described as follows:

$$\begin{cases} E_0 = (0, 0, 0) \\ E_{\pm} = (\pm c, 0, \mp c) \end{cases} \quad (7)$$

Where c is the solution of the transcendental equation:

$$(a-1)c - 0.5b(\exp(kc) - \exp(-c)) = 0 \quad (8)$$

Using the MATLAB build-in function and the set of parameters of the particular case the solution of (8) yields. This solution is in accordance with the results since the graph in black which represents the case $k=1$ intersects the x -axis at ± 8.77343 (Figure 3).

The Jacobian matrix at the various equilibriums is defined as:

$$\begin{pmatrix} \alpha(a-1-0.5b(k\exp(k\mu) + \exp(-\mu))) & \alpha & 0 \\ 1 & -1 & 1 \\ 0 & -\beta & 0 \end{pmatrix} \quad (9)$$

With for the zero fixed point; for the non-zero equilibriums. The

Eigen values related to the above matrix can be found by solving the following characteristics equations:

$$\lambda^3 + a_2\lambda^2 + a_1\lambda + a_0 = 0$$

where

$$\begin{cases} a_0 = \alpha\beta(1-a+0.5bk\exp(ck)+0.5b\exp(-c)) \\ a_1 = \alpha(-a+0.5bk\exp(ck)+0.5b\exp(-c))+\beta \\ a_2 = \alpha(1-a+0.5bk\exp(ck)+0.5b\exp(-c))+1 \end{cases}$$

For the particular case $k=1$; $\alpha=5.892857$; $\beta=6.6$; $a=1.111111$ $b=3.017867 \times 10^{-4}$ the Routh–Hurwitz criterion is not satisfied for the zero equilibrium implying that the latter is always unstable whereas the non-zero equilibriums are stable [36].

Numerical Results and Discussions

To scan the dynamics of the generalized Chua's circuit under consideration, the fourth order R-K algorithm has been used to solve system (4) with a small integration step. The transient is eliminated during the integration. The main indicator used to demonstrate the phenomenon of multistability is the coexisting bifurcation diagrams. Note these diagrams are obtained by plotting the local maximums of the variable versus a given control parameter. The largest lyapunov exponents are also used to characterize the system's dynamics [37-39].

Coexisting bifurcations and coexisting attractors in the particular case ($k=1$)

In this section we make a brief recall of the results presented by Bao and coworker [33]. To this end, we fixed $k=1$; $a=1.111111$; $b=3.017867 \times 10^{-4}$; $\beta=6.6$ and increase α in the range $5.5 < \alpha < 6.7$. The system is solved with various initial states leading to coexisting bifurcations (Figure 4). The graphs in green and black colours are the bifurcations of the two nonzero fixed points. These diagrams are obtained from the initial states $(\pm 8; 0; \mp 8)$. A limit cycle is obtained by solving the system with $(0; 8; 0)$. The corresponding bifurcation diagram is represented in magenta colour. When the initial conditions $(0; \mp 0.001; 0)$ are chosen, two different routes coexist where periodic attractors coexist at the same point and chaotic attractors coexist at the same point. The corresponding bifurcation diagrams are provided in blue and

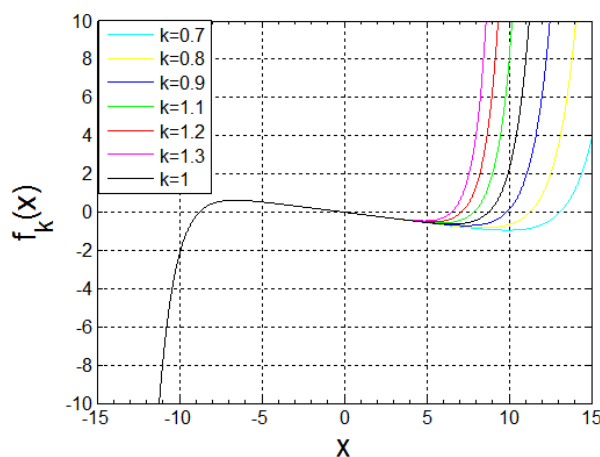
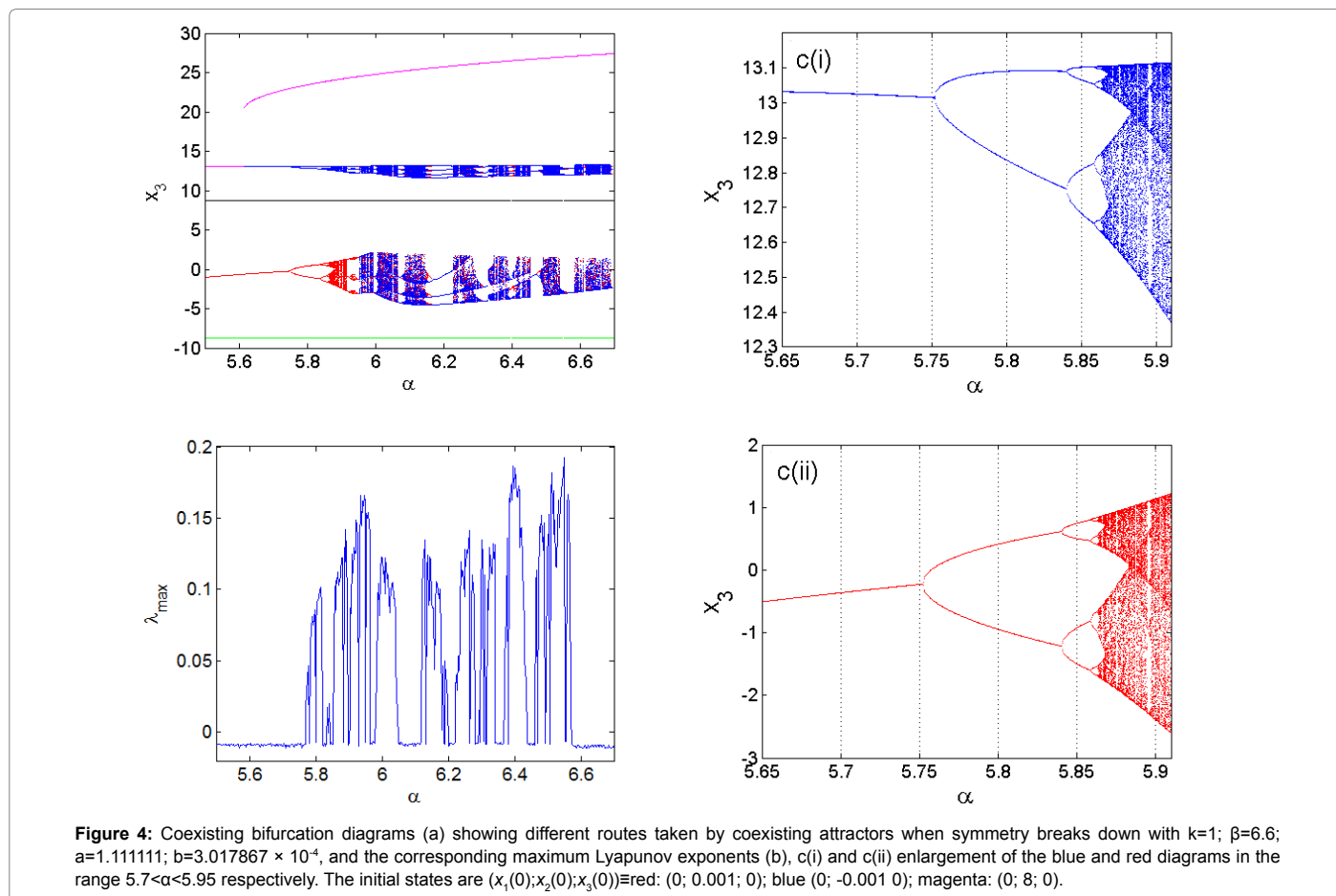


Figure 3: The nonlinear function $f_k(x)$ for various values of the parameter k . Notice that for $k=1$ the system displays two symmetric fixed points, but for $k \neq 1$ the fixed points are no more symmetric.



red colour with an enlargement (Figure 4). Under these conditions, it is obvious that the system moves from periodic to chaotic attractors with a period doubling bifurcation. The largest Lyapunov exponent can also attest this dynamics (Figure 4). In addition the different routes lead to a symmetric double scroll attractor. For illustration the graph of Figure 5 is provided with the projection of the symmetric double-scroll chaotic attractor (a), (b), (c) and the corresponding double-sided Poincaré section (d) in the plane $x_1=0$; for $\alpha=6.1$. Various phase portraits are plotted for different values of the parameter α to illustrate the coexistence of point attractors, limit cycles and chaotic attractors (Figure 6).

Coexisting bifurcations and coexisting attractors in the particular case ($k \neq 1$)

This section is devoted to the analysis of the generalized Chua's circuit: $k \neq 1$. We use k as the control parameter in the range $0.4 < k < 1.2$; the rest of parameters being fixed as $\alpha=5.892857$; $\beta=6.6$; $a=1.111111$; $b=3.017867 \times 10^{-4}$. With these parameters the system is solved with various initial conditions and coexisting bifurcation is achieved (Figure 5). Figure 7 is an illustration where the graphs in red and blue colours are obtained by setting the initial conditions $(0, \pm 0.01, 0)$. From these diagrams it is obvious that a spiral chaotic attractor (graph in red colour) always coexist for the set of parameters above mentioned. Beside we have a period doubling bifurcation (graph in blue colour) leading to different spiral chaotic attractor. The systems dynamics transit from periodic to chaotic behaviour. Several periodic windows intersect the chaotic region. With $(0, -8, 0)$ and $(20, 0, 20)$

as initial states, the system yields the graphs in magenta and green colours where a limit cycle and points attractors are obtained. Note that the amplitude of the limit cycle decreases as parameter k increases. In addition, the system has two stable point attractors. One of them is always located at $x_1=8.77343$ and the coordinate of the second one decreases as parameter k increases. This observation confirms the results presented (Figure 3).

Various phase portraits are plotted in the (x_1, x_2) plane for different values of parameter k showing different kinds of coexisting attractors of point attractors, limit cycles and spiral chaotic attractors (Figures 8-10). The case $k=0.8$ has been explored in deep by controlling the system with parameter α in the range $5.5 < \alpha < 6.7$ with $\beta=6.6$, $a=1.111111$; $b=3.017867 \times 10^{-4}$. For this set of parameter system (6) experience five coexisting bifurcations and thus five coexisting attractors: a limit cycle, two asymmetric point attractors and two period doubling routes to asymmetric double scroll chaotic attractor. Figure 11 is the representation of the symmetric double scroll chaotic attractor and the corresponding double-sided Poincaré section (d) in the plane $x_1=0$; for $\alpha=6.1$. A similar study has been carried out for $k=1.2$ (Figure 12). The coexisting bifurcation and the corresponding coexisting attractors are shown respectively (Figures 13 and 14). For a kind of coexisting attractor ($k=0.8$, $\alpha=6.1$, $\beta=6.6$, $a=1.111111$, $b=3.017867 \times 10^{-4}$) the cross section of the basin of attraction has been plotted where the region in red represents the basin of attraction of the asymmetric double scroll chaotic attractor, the regions in cyan and purple colours represents the basin of point attractors. The yellow represent the region of limit cycle. Note that the limit cycle is a hidden attractor since its basin

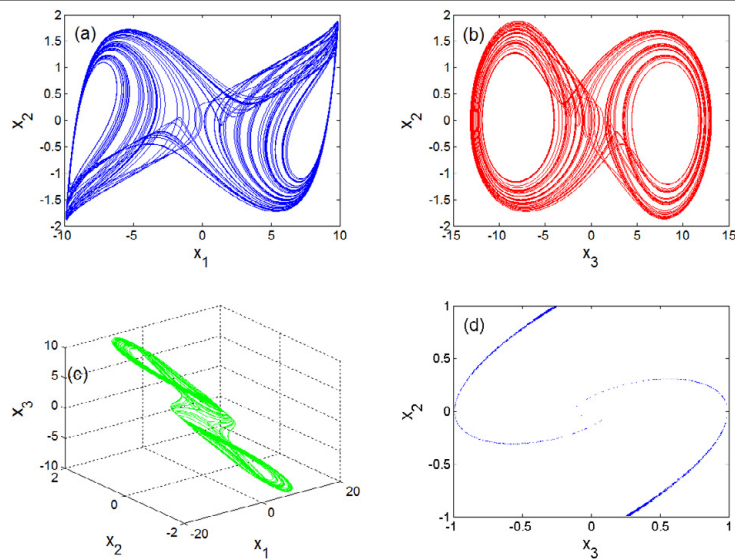


Figure 5: Projection of the Double-Scroll Chaotic Attractor (a), (b), (c) and the corresponding double-sided Poincaré section (d) in the plane $x_1=0$: for $k=1$ and the rest of system parameter set as $\beta=6.6$; $\alpha=6.1$; $a=1.111111$; $b=3.017867 \times 10^{-4}$. The attractor is perfectly symmetric.

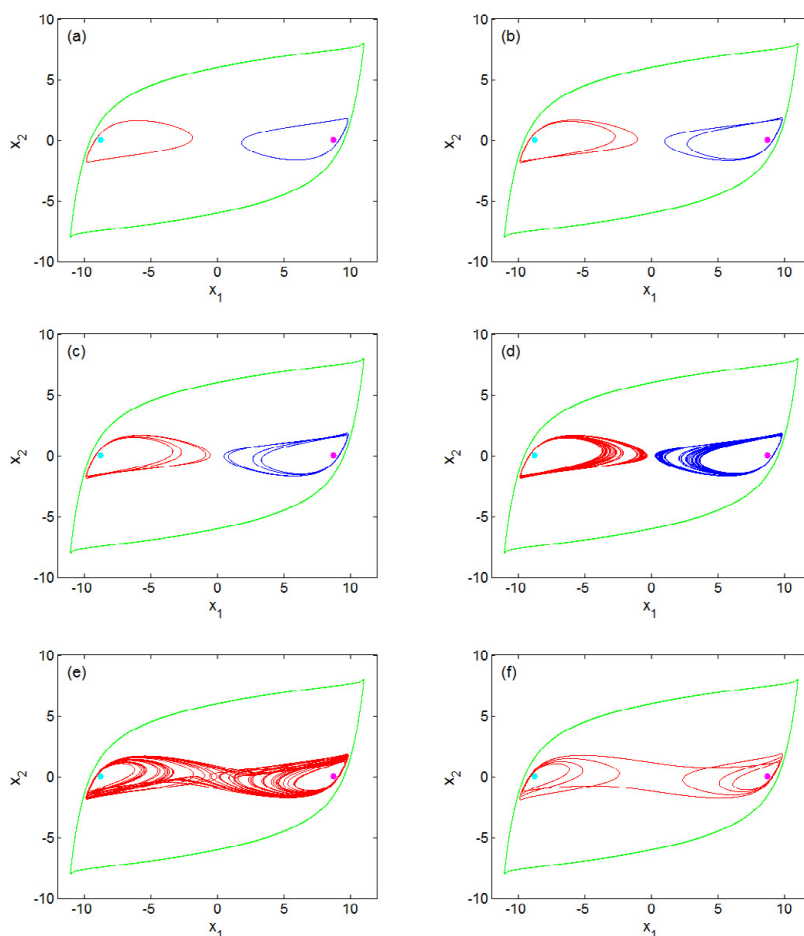


Figure 6: Numerical coexisting attractors with different values of α in the x - y plane, $k=1$; $\beta=6.6$; $a=1.111111$; $b=3.017867 \times 10^{-4}$, Limit cycles and fixe point attractor for $\alpha=5.66$. (a)Limit cycles and fixe point attractor for $\alpha=5.8$, (b) Limit cycles and fixe point attractor for $\alpha=5.879$, (c) Spiral chaotic attractor, limit cycle and fixe point attractor for $\alpha=5.879$, (d) Spiral chaotic attractor, limit cycle and fixe point attractor for $\alpha=5.879$, (e) Double-scroll chaotic attractor, limit cycle and fixe point attractor for $\alpha=6.1$, (f) Limit cycles and fixe point attractor for $\alpha=6.2$. The initial state are $(x_1(0);x_2(0);x_3(0))$: red: (0;0.001;0); blue: (0;-0.001;0); green (0;8;0); magenta: (-8;0;8);cyan: (8;0;8).

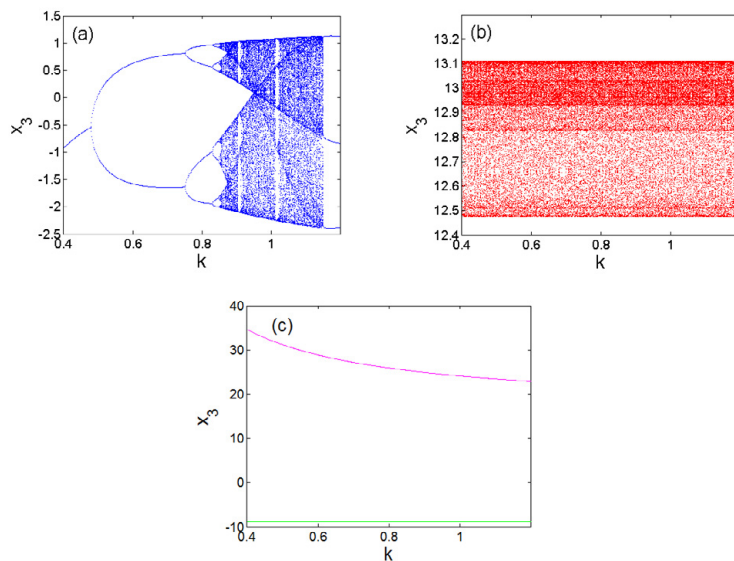


Figure 7: Dynamics of system (6) versus the control parameter k for different initial states: $(x_1(0);x_2(0);x_3(0))$ =red; (0;0.001;0); blue: (0;-0.001; 0); magenta: (-8; 0;8); green (0; 8; 0); black: (-8 0;8).

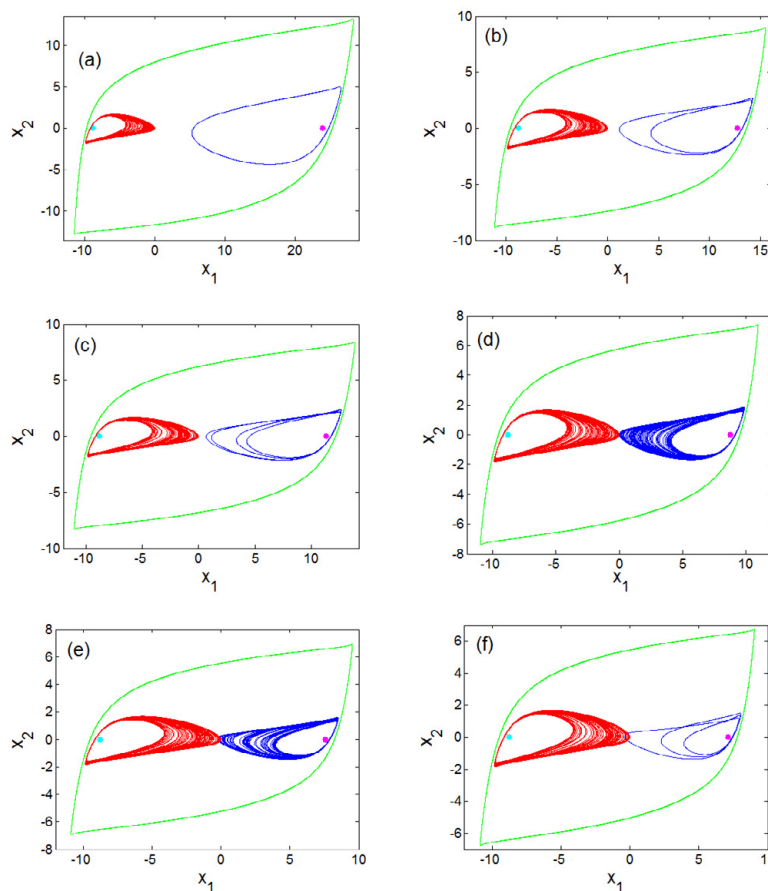


Figure 8: Numerical coexisting attractors with different values of k in the x - y plane, $\alpha=5.892857$; $\beta=6.6$; $a=1.111111$; $b=3.017867 \times 10^{-4}$. (a) Spiral chaotic attractor, Limit cycles and fixe point attractor for $k=0.41$, (b) Spiral chaotic attractor, Limit cycles and fixe point attractor for $k=0.72$, (c) Spiral chaotic attractor, Limit cycles and fixe point attractor for $k=0.8$, (d) Spiral chaotic attractors, limit cycle and fixe point attractor for $k=1$, (e) Spiral chaotic attractors, limit cycle and fixe point attractor for $k=1.14$, (f) Spiral chaotic attractors, Limit cycles and fixe point attractor for $k=1.2$. The initial sate are $(x_1(0);x_2(0);x_3(0))$ =red; (0;0.001;0); blue: (0;-0.001; 0); green (0; -8; 0); magenta: (20; 0;-20);cyan: (8 0;8),for (a) and $(x_1(0);x_2(0);x_3(0))$ =red; (0;0.001;0); blue: (0;-0.001; 0); green (-8;0;8); magenta: (8; 0;-8); cyan: (-8 0;8) for the rest.

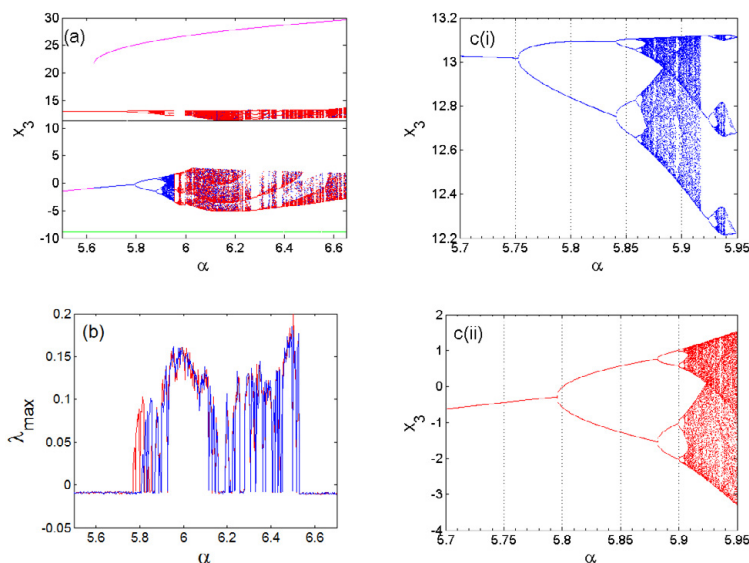


Figure 9: Coexisting bifurcation diagrams (a) showing different routes taken by coexisting attractors when symmetry breaks down with, and the corresponding maximum Lyapunov exponents (b). c(i) and c(ii) are the enlargement of the blue and red diagrams in the range $5.7 < \alpha < 5.95$ respectively. The initial state are $(x_1(0); x_2(0); x_3(0)) =$ red: $(0; 0.001; 0)$; blue: $(0; -0.001; 0)$; magenta: $(0.8; 0)$; green $(-8; 0; 8)$; black: $(8; 0; -8)$.

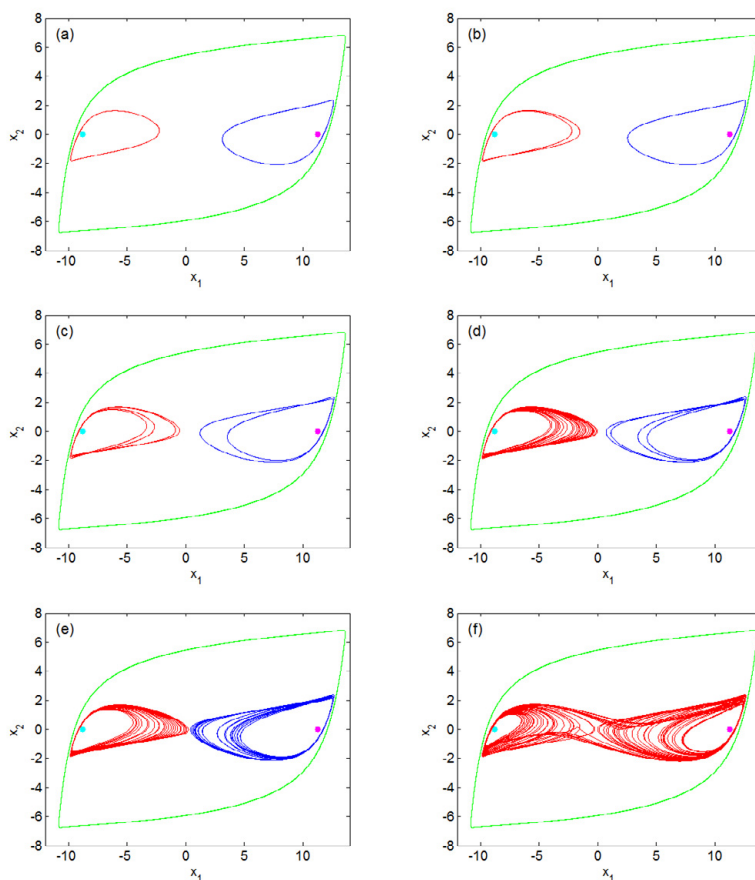


Figure 10: Numerical coexisting attractors with different values α of in the x_1 - x_2 plane, $k=0.8$; $\beta=6.6$; $a=1.111111$; $b=3.017867 \times 10^{-4}$. (a) Limit cycles and fix point attractor for $\alpha=5.69$, (b) Limit cycles and fix point attractor for $\alpha=5.778$, (c) Limit cycles and fix point attractor for $\alpha=5.855$, (d) Spiral chaotic attractor, limit cycle and fix point attractor for $\alpha=5.94$, (e) Spiral chaotic attractor, limit cycle and fix point attractor for $\alpha=5.913$, (f) Double-scroll chaotic attractor, limit cycle and fix point attractor for $\alpha=6.1$. The initial state are $(x_1(0); x_2(0); x_3(0)) =$ red: $(0; 0.001; 0)$; blue: $(0; -0.001; 0)$; green $(0.8; 0)$; magenta: $(-8; 0; 8)$; cyan: $(8; 0; -8)$.

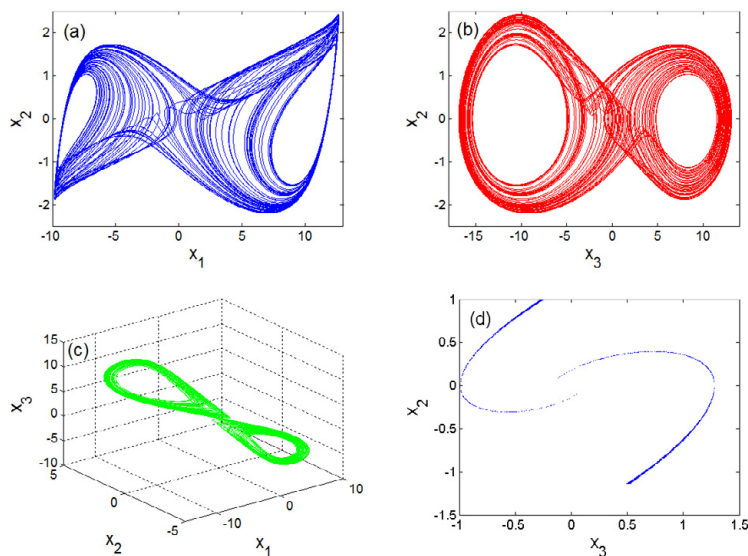


Figure 11: Projection of the Double-Scroll Chaotic Attractor (a), (b), (c) and the Corresponding Double-Sided Poincaré Section (d) in the plane $x_1=0$: for $k=0.8$ and the rest of system parameter set as $\beta=6.6$; $\alpha=6.1$; $a=1.111111$; $b=3.018776 \times 10^{-4}$. The attractor is not symmetric.

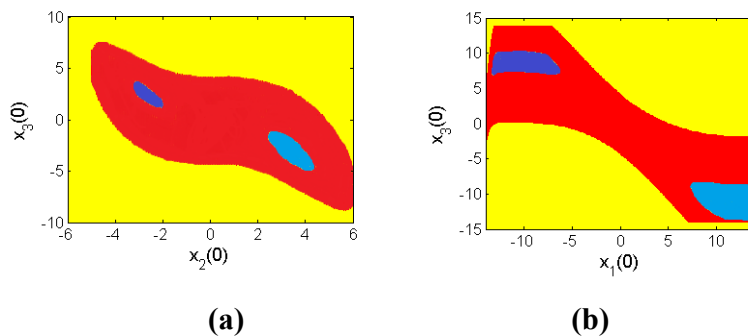


Figure 12: Cross Sections of the Basin of Attraction with $x_1(0)=0$ and $x_2(0)=0$ corresponding to two Different Parameters of Coexisting Attractors presented in figure: 10 (f) $\alpha=6.1$.

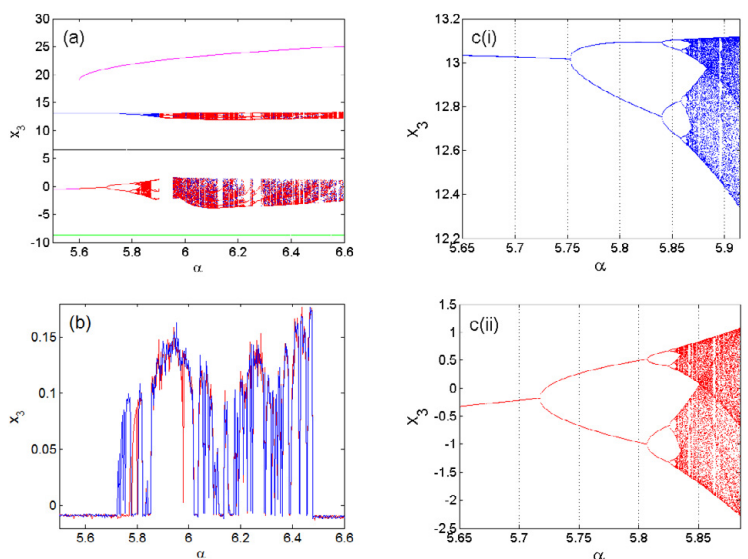


Figure 13: Coexisting Bifurcation Diagrams (a) showing Different Routes taken by Coexisting Attractors when Symmetry breaks down with $k=1.2$; $\beta=6.6$; $a=1.111111$; $b=3.017867 \times 10^{-4}$, and the Corresponding Maximum Lyapunov Exponents (b). c(i) and c(ii) are the Enlargement of the blue and Red Diagrams in the range $5.65 < \alpha < 5.915$ respectively. The Initial State are $(x_1(0); x_2(0); x_3(0)) =$ red: $(0; 0.001; 0)$; blue: $(0; -0.001; 0)$; magenta: $(0; 8; 0)$; green $(-8; 0; 8)$; black: $(8; 0; -8)$.

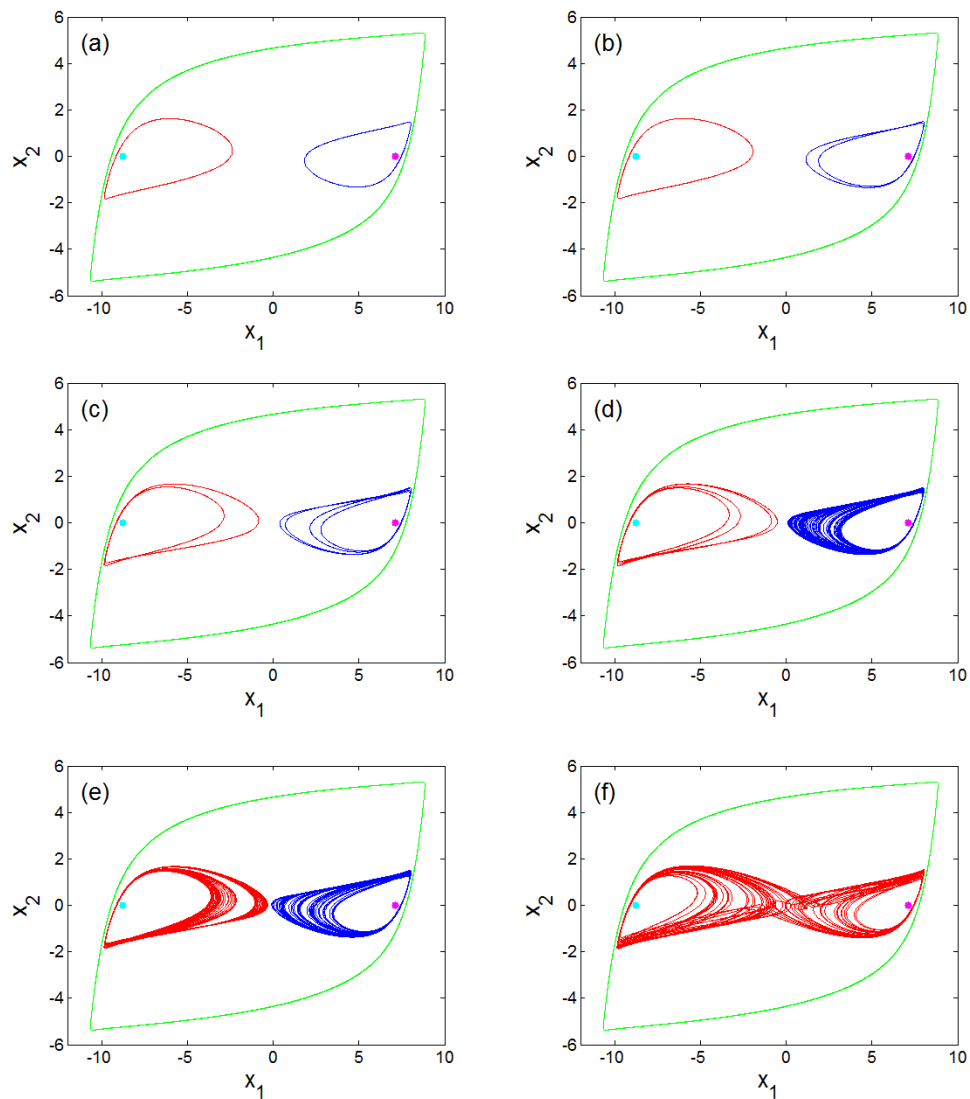


Figure 14: Numerical Coexisting Attractors with different values of α in the x - y plane, $k=1.2$; $\beta=6.6$; $a=1.111111$; $b=3.017867 \times 10^{-4}$. (a) Limit cycles and fixe point attractor for $\alpha=5.68$, (b) Limit cycles and fixe point attractor for $\alpha=5.82$, (c) Limit cycles and fixe point attractor for $\alpha=5.85$, (d) Spiral chaotic attractor, limit cycle and fixe point attractor for $\alpha=6$, (e) Double-scroll chaotic attractor, limit cycle and fixe point attractor for $\alpha=6$, (f) Limit cycles and fixe point attractor for. The initial sate are $(x_1(0);x_2(0);x_3(0))$ ≡red: (0;0.001;0); blue: (0;-0.001; 0); green: (0; 8;0); magenta (-8;0;8); cyan: (8; 0; -8).

of attraction does not intersect with small neighbourhoods of three equilibrium points of system (6) [40,41].

Let us stress that multistability has multiple fields of application and as such the phenomenon has been extensively revealed in nonlinear dynamical systems [1-18].

Pspice Simulation Results

According to the above numerical analysis, the generalized Chua's circuit experiences the striking dynamics of coexisting attractors. To verify this dynamics the circuit of Figure 1 is simulated under Pspice software with the Chua's diode of the following components values are used (Figure 2):

$$C_2=33n, L=20mH, R=2K, R_f=R==1.8K, R_0=400K, kR_0=320K(k=0.8).$$

For $C_1=6nF$, three limit cycles coexist and the initial states are

$$(v_{c1}(0), v_{c2}(0), i_L(0))=(0, \pm 0.001, 0) \text{ and } (v_{c1}(0), v_{c2}(0), i_L(0))=(0, 8, 0)$$

(Figure 15).

For $C_1=5.72nF$, three limit cycles coexist and the initial states are $(v_{c1}(0), v_{c2}(0), i_L(0))=(0, \pm 0.001, 0)$ and $(v_{c1}(0), v_{c2}(0), i_L(0))=(0, 8, 0)$ (Figure 16).

For $C_1=6nF$ three limit cycles coexist and the initial states are $(v_{c1}(0), v_{c2}(0), i_L(0))=(0, 0.001, 0)$ and $(v_{c1}(0), v_{c2}(0), i_L(0))=(0, 8, 0)$ (Figure 17).

With regard to coexisting attractors, a very good similarity can be observed between the numerical phase portrait of the circuit's model and the PSpice phase portrait of the real circuit (Figure 1). However, some slight differences can be noticed between the numerical and the PSpice simulation results. These differences should be attributed in part to the precision on the values of electronic components as well as simplifying assumptions considered during the modelling process of the circuit.

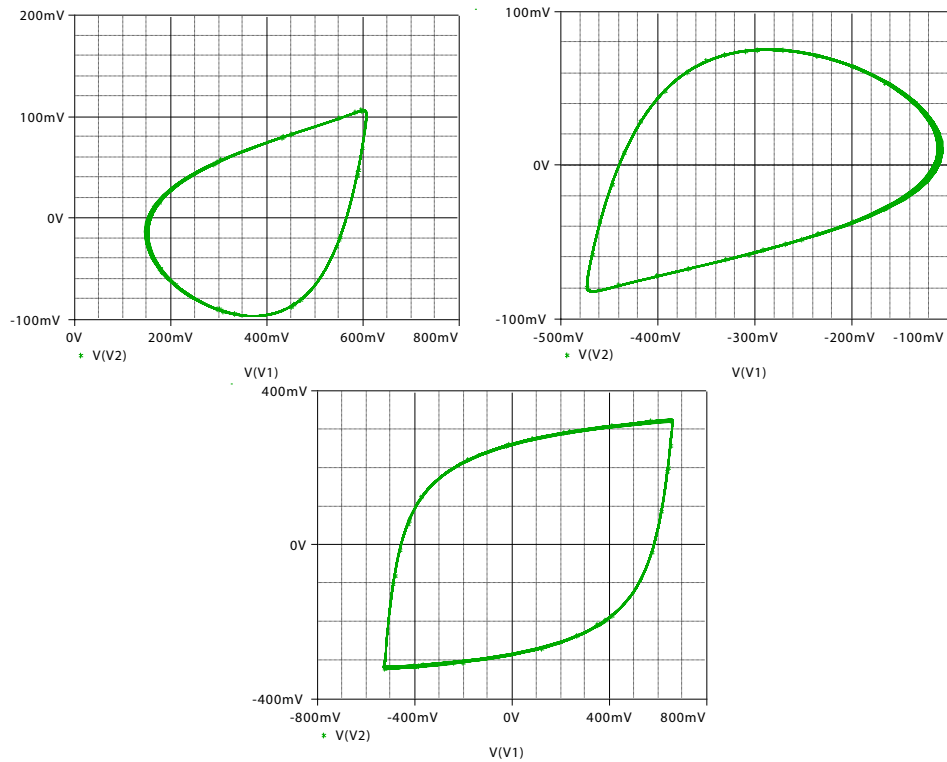


Figure 15: PSpice simulation results showing the coexistence of three limit cycles for: $C_1=6 \text{ nF}$; The Initial Conditions are $(u_{C_1}(0), u_{C_2}(0), i_L(0))=(0, \pm 0.001)$ and $(u_{C_1}(0), u_{C_2}(0), i_L(0))=(0, 8, 0)$. $C_1=6, C_2=33 \text{ n}, L=20 \text{ mH}, R=2\text{k}, R_f=R_3=1.8\text{K}, R_0=400\text{K}, kR_0=320\text{K}, k=0.8$.

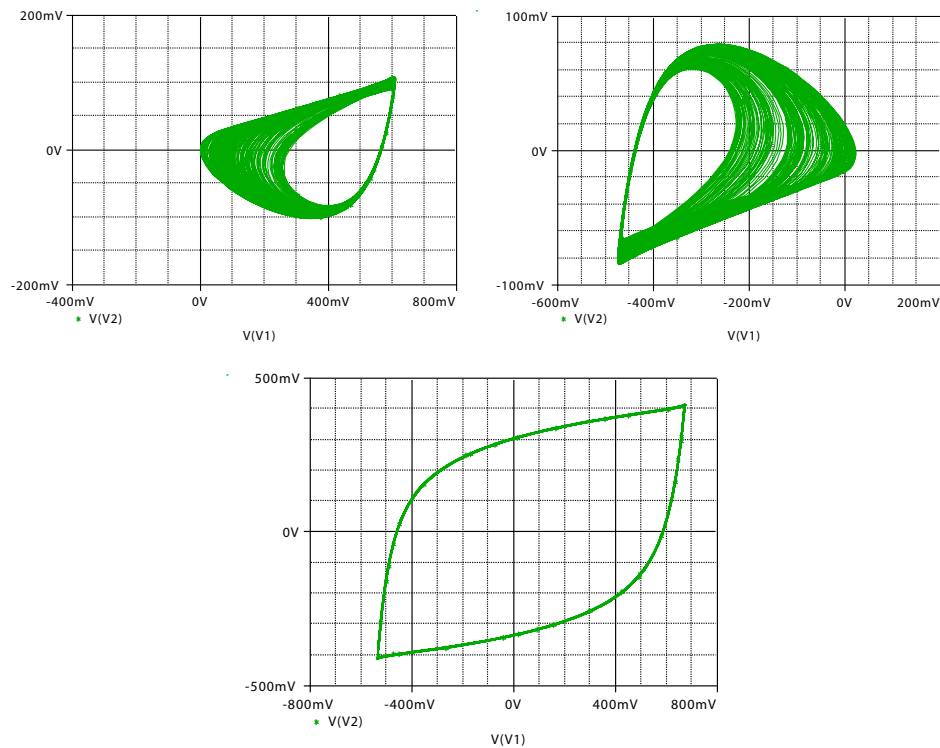
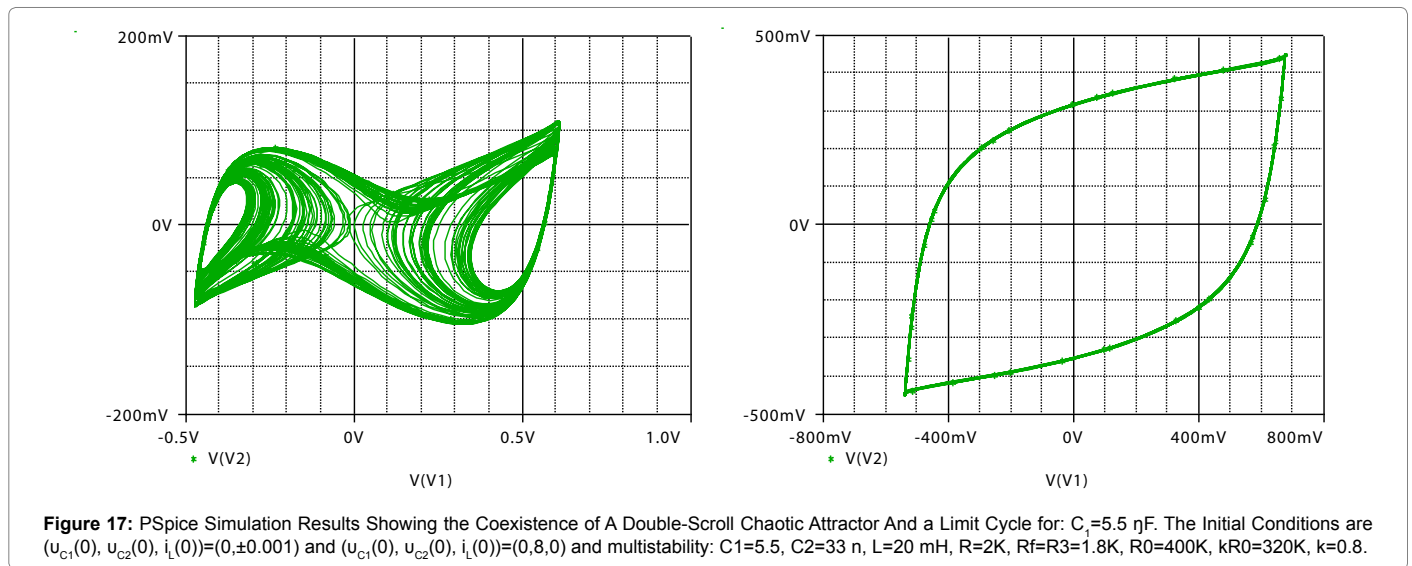


Figure 16: PSpice Simulation Results showing the Coexistence of two Chaotic Spiral Attractors and a Limit Cycle for: $C_1=5.72 \text{ nF}$. The Initial Conditions are $(u_{C_1}(0), u_{C_2}(0), i_L(0))=(0, \pm 0.001)$ and $(u_{C_1}(0), u_{C_2}(0), i_L(0))=(0, 8, 0)$. Multistability: $C_1=5.72, C_2=33 \text{ n}, L=20 \text{ mH}, R=2\text{K}, R_f=R_3=1.8\text{K}, R_0=400\text{K}, kR_0=320\text{K}, k=0.8$.



Conclusion

This paper has investigated a generalized Chua's circuit. The circuit is obtained by replacing the Chua's diode of a classical Chua's circuit with an adjustable Chua's diode modelled by $f_k(x_1)=-ax_1+b(\exp(kx_1)-\exp(-x_1))$. The stability analysis shows that the system has two stable nonzero fixed points. In addition the system is symmetric for the particular case. In this case the system displays complex nonlinear phenomena such as the symmetry breaking in which a symmetric pair of attractors coexists and merges into one symmetric attractor through an attractor-merging bifurcation. When $k \neq 1$ the symmetry breaks down but its complex dynamics remain complex with the coexistence of point attractors, limit cycles, chaotic spiral attractors and double scroll chaotic attractors. In contrast to the case $k=1$, two asymmetric chaotic spiral attractors coexist and merge into one asymmetric double scroll chaotic attractor. For a kind of coexisting attractors the cross section of the basins of attraction of the various coexisting attractors has been plotted. More importantly, multistability in the symmetry boundary is discussed by switching the control parameter k . The result shows that the limit cycle is a hidden attractor since its basin of attraction does not intersect with small neighbourhoods of three equilibrium points of system (6) [40,41]. The Pspice simulation results support the numerical simulations.

References

- Kengne J, Tsafack N, Kamdjeu L Dynamical Analysis of a Novel Single Opamp-Based Autonomous LC Oscillator: Antimonotonicity, Chaos, and Multiple Attractors. *Int J Dyn Control* 6: 1543-1557.
- Lai Q, Tsafack N, Kengne J, Zhao XW (2018) Coexisting Attractors and Circuit Implementation of a New 4D Chaotic System with Two Equilibria. *Chaos, Solitons and Fractals* 107: 92-102.
- Kengne J, Nguomkam Negou A, Njitacke ZT (2017) Antimonotonicity, Chaos and Multiple Attractors in a Novel Autonomous Jerk Circuit. *Int J Bifurc Chaos* 88: 2589-2608.
- Kengne J, Folifack V, Chedjou J, Leutcho G (2017) Nonlinear Behavior of a Novel Chaotic Jerk System: Antimonotonicity, Crises, And Multiple Coexisting Attractors. *Int J Dyn Control* 6: 468-485.
- Fozin TF, Srinivas K, Kengne J, Pelap FB (2018) Coexisting Bifurcations in a Memristive Hyperchaotic Oscillator. *AEU - Int J Electron Commun* 90: 110-122.
- Li C, Hu W, Sprott JC, Wang X (2015) Multistability in Symmetric Chaotic Systems. *Eur Phys J Special Topics* 224: 1493-1506.
- Sajad J, Atefeh A, Abdul JMK, Hamid RA, Pham VT, et al. (2018) A New Hidden Chaotic Attractor with Extreme Multi-Stability. *AEU - Int J Electron Commun* 89: 131-135.
- Li C, Sprott JC (2014) Coexisting Hidden Attractors in a 4-D Simplified Lorenz System. *Int J Bifurcation Chaos* 24: 1450034.
- Rajasekar S, Lakshmanan M (1990) Multiple Attractors and their Basins of Attraction of a Long Josephson Junction Oscillator. *Phys Lett A* 147: 264-8.
- Bao B, Xu Q, Bao H, Chen M (2016) Extreme Multistability in a Memristive Circuit. *Electron Lett* 52: 1008-1010.
- Nguomkam A.N, Kengne J Dynamic Analysis of a Unique Jerk System with a Smoothly Adjustable Symmetry and Nonlinearity: Reversals of Period Doubling, Offset Boosting and Coexisting Bifurcations. *AEU - Int J Electron Commun* 90: 1-19.
- Jaros P, Perlikowski P, Kapitaniak T (2015) Synchronization and Multistability in the Ring of Modified R'ossler Oscillators. *Eur Phys J* 224: 1541-1552.
- Li B, Hu W, Sprott JC, Wang X (2015) Multistability in Symmetric Chaotic Systems. *Eur Phys J S* 224: 1493-1506.
- Leipnik RB, Newton TA (1981) Double Strange Attractors in Rigid Body Motion with Linear Feedback Control. *Phys Lett A* 86: 63-87.
- Nguimdo RM, Tchitinga R, Woafu P (2013) Dynamics of Coupled Simplest Chaotic Two Component Electronic Circuits and its Potential Application to Random Bit Generation. *Chaos* 23: 043122.
- Hong Z, Xieting L (1997) Generating Chaotic secure sequences with desired Statistical Properties and high Security. *Int J Bifurcation and Chaos* 7: 205- 213.
- Bernstein GM, Lieberman MA (1990) Secure Random Number Generation using Chaotic Circuits. *IEEE Trans Circuits and Systems* 37: 1157-1164.
- Bao BC, Hu FW, Chen M, Xu Q (2015) Self Excited and Hidden Attractors Found Simultaneously in a Modified Chua's Circuit. *Int J Bifurcation and Chaos* 25: 1-10.
- Bao BC, Jiang P, Xu Q, Chen M (2016) Hidden Attractors in a Practical Chua's Circuit Based on a Modified Chua's Diode. *Electron Lett* 52: 23-25.
- Bao BC, Li QD, Wang N, Xu Q (2016) Multistability in Chua's Circuit with two Stable Node-Foci Chaos. *26: 043111*.
- Chen M, Yu JJ, Bao BC (2015) Hidden Dynamics and Multi-Stability in an Improved third Order Chua's Circuit. *J Eng* 87.
- M, Xu Q, Lin Y, Bao BC (2017) Multistability Induced by Two Symmetric Stable Node-Foci in Modified Canonical Chua's Circuit. *Nonlin Dyn* 87: 789-802.
- Elwakil AS, Kennedy MP (2000) Improved Implementation of Chua's Chaotic Oscillator using Current Feedback Op Amp. *IEEE Trans Circuits Syst -I* 47: 76-79.

24. Li QD, Zeng HZ, Yang XS (2014) On Hidden Twin Attractors and Bifurcation in the Chua's Circuit. *Nonlin Dyn* 77: 255-266.
25. Xu Q, Lin Y, Bao BC, Chen M (2016) Multiple Attractors in a Non-Ideal Active Voltage-Controlled Memristor Based Chua's Circuit. *Chaos Solit Fract* 83: 186-200.
26. Yalcin ME, Suykens JAK, Vandewalle J (2000) Experimental Confirmation of 3-and 5-Scroll Attractors from a Generalized Chua's Circuit. *IEEE Trans Circuits Syst-I* 47: 425-429.
27. Matsumoto T (1984) A Chaotic Attractor from Chua's Circuit. *IEEE Trans Circuits Syst CAS-31*: 1055-1058.
28. Matsumoto T, Chua LO, Komuro M (1985) The double scroll. *IEEE Trans. Circuits Syst. CAS-32*: 797-818.
29. Matsumoto T, Chua LO, Komuro M (1986) Double scroll Via a Two-Transistor Circuit. *IEEE Trans Circuits Syst CAS* 33 828-835.
30. Kennedy MP (1992) Robust Op Amp Realization of Chua's Circuit. *Frequenz* 46: 66-80.
31. Arena P, Baglio S, Fortuna L, Manganaro G (1995) Chua's circuit can be generated by CNN Cells. *IEEE Trans. Circuits Syst -I* 42; 123-125.
32. Bao B, Huagan W, Li X, Mo C (2018) Coexistence of Multiple Attractors in an Active Diode Pair Based Chua's Circuit. *Int J Bifurcation Chaos* 28: 1850019.
33. Haniyas MP, Giannaris G, Spyridakis AR (2006) Time Series Analysis in Chaotic Diode Resonator Circuit. *Chaos. Solitons and Fractals* 27: 569.
34. Sukov DW, Bleich ME, Gauthier J, Socolar JES (1997) Controlling Chaos in a Fast Diode Resonator Using Extended Time-Delay Auto-Synchronization: Experimental Observations and Theoretical Analysis. *Chaos* 7: 560.
35. Strogatz SH (1994) *Nonlinear Dynamics and Chaos*. Reading Addison-Wesley.
36. Wolf A, Swift JB, Swinney HL, Wastano JA (1985) Determining Lyapunov Exponents From Time Series. *Physica D* 16: 285-317.
37. Fredeiuickson P, Kaplan JL, Yorke ED, Yorke JA (1983) The Liapunov Dimension of Strange Attractors. *J Diff Equations* 49: 185-207.
38. Kuznetsov NV, Leonov GA, Mokaev TN, Prasad A, Shrimal MD (2018) Finite-time Lyapunov Dimension and Hidden Attractor of the Rabinovich System. *Nonlinear Dyn* 92: 267-285.
39. Leonov GA, Kuznetsov NV, Vagaitsev VI (2011) Localization of Hidden Chua's Attractors. *Phys Lett A* 375: 2230-2233.
40. Leonov GA, Kuznetsov NV, Mokaev TN (2015) Hidden Attractor and Homoclinic Orbit in Lorenz-like System Describing Convective Fluid Motion in Rotating Cavity. *Commun Nonlin Sci Numer Simulat* 28: 166-174.
41. Kuznetsov NV, Leonov GA, Yuldashev MV, Yuldashev RV (2017) Hidden Attractors in Dynamical Models of Phase-Locked Loop Circuits: Limitations of Simulation in MATLAB and SPICE. *Comm in Nonlinear Sc a Numer Simulat*.